Received: 8 April 2021 | Revised: 28 July 2021 | Accepted: 6 August 2021

DOI: 10.1111/cas.15104

ORIGINAL ARTICLE

Cancer Science WILEY

ELF3-AS1 contributes to gastric cancer progression by binding to hnRNPK and induces thrombocytosis in peripheral blood

Shubin Song[1,2] | Xuezhi He[3] | Jing Wang[4] | Rong Wang[5] | Leilei Wang[2] | Wei Zhao[2] | Yimin Wang[1] | Yongle Zhang[1] | Zhiyong Yu[2] | Dengshun Miao[6] | Yingwei Xue[1]

[1]Department of gastrointestinal surgery, Harbin Medical University Cancer Hospital, Harbin, China

[2]Department of Breast Surgery, Shandong Cancer Hospital and Institute, Shandong First Medical University and Shandong Academy of Medical Sciences, Jinan, China

[3]Department of Nutrition and Food Hygiene, School of Public Health, Nanjing Medical University, Nanjing, China

[4]Department of Anatomy, Histology and Embryology, State Key Laboratory of Reproductive Medicine, The Research Center for Bone and Stem Cells, Nanjing Medical University, Nanjing, China

[5]Department of Anatomy, Histology and Embryology, The Research Center for Bone and Stem Cells, Nanjing Medical University, Nanjing, China

[6]The Research Center for Aging, Friendship Affiliated Plastic Surgery Hospital of Nanjing Medical University, Nanjing, China

Correspondence
Yingwei Xue, Department of gastrointestinal surgery, Harbin Medical University Cancer Hospital, Harbin, China.
Email: xyw801@163.com

Dengshun Miao, The Research Center for Aging, Friendship Affiliated Plastic Surgery Hospital of Nanjing Medical University, Nanjing, China.
Email: dsmiao@njmu.edu.cn

Zhiyong Yu, Department of Breast Surgery, Shandong Cancer Hospital and Institute, Shandong First Medical University and Shandong Academy of Medical Sciences, Jinan, China.
Email: drzhiyongyu@aliyun.com

Funding information
Harbin Science and Technology Bureau Research and Development Project of Applied Technology, Grant/Award Number: 2017RAXXJ054; Nn10 program of Harbin Medical University Cancer Hospital (Nn 10PY2017-03); the Grants from the National Natural Science Foundation of China, Grant/Award Number: 81730066; the Grants from the Natural Science Foundation of Shandong Province, Grant/Award Number: ZR2019MH109

Abstract

Numerous studies have reported that a variety of long noncoding RNAs (lncRNAs) can promote the proliferation, invasion, and migration of different tumor cells. However, different lncRNAs regulate cell functions in various forms, and the exact mechanisms are not clear. Here, we investigated the effect of the lncRNA ELF3-AS1 on gastric cancer (GC) cell function and explored the exact mechanism. Quantitative real-time polymerase chain reaction was used to detect the expression of ELF3-AS1 in GC tissues and adjacent nontumor tissues. Knockdown and overexpression of ELF3-AS1 was used to detect the effect of ELF3-AS1 on cell function. Potential downstream target genes were identified using RNA transcriptome sequencing, while RNA immunoprecipitation, chromatin immunoprecipitation, and Western blotting were performed to explore the tumor promotion mechanisms of ELF3-AS1. We observed that ELF3-AS1 was highly expressed in GC tissues, and high ELF3-AS1 expression predicted poor prognosis. The knockdown of ELF3-AS1 significantly inhibited cell proliferation, migration, and epithelial-mesenchymal transition and promoted apoptosis. Mechanistic investigations revealed that ELF3-AS1 may regulate the downstream target gene, C-C motif chemokine 20, by binding with the RNA-binding protein hnRNPK. Additionally, we found that high ELF3-AS1 expression was associated with thrombocytosis. Interleukin-6 and thrombopoietin may be involved in ELF3-AS1–induced paraneoplastic thrombocytosis. Together, our results demonstrate that

Song and He contributed equally to the article.

aberrantly expressed ELF3-AS1 in GC may play important roles in oncogenesis and progression and is expected to become a new target for the diagnosis and treatment of GC.

KEYWORDS
gastric cancer, hnRNPK, lncRNA, platelet

1 | INTRODUCTION

Gastric cancer (GC) is a high-incidence malignant tumor of the digestive system that is induced by multiple factors such as environment, diet, *Helicobacter pylori* infection, and genetic mutations.[1] There is increasing difficulty with using traditional open surgery, laparoscopic surgery, endoscopic surgery, and chemotherapy to improve the prognosis of patients with GC. Attempts have been made to improve the prognosis of patients by the targeted treatment of GC genes and at the molecular level. With the completion of human genome engineering and the development of high-throughput sequencing technology, research on the gene development of tumors has gradually gained attention, especially long noncoding RNAs (lncRNAs). Encoded RNA accounts for only about 2% of the genome, and more than 90% of the genomic DNA can be transcribed into noncoding RNAs (ncRNAs), including small ncRNAs (less than 200 bp) and lncRNAs (longer than 200 bp).[2-4] Initially, lncRNA was considered as spurious noise of genomic transcription, but with deeper research into lncRNA functions, it was found that lncRNAs are not only expressed and distributed in specific tissues and cells but also play important roles in gene transcription and protein expression.[5]

Numerous studies have reported that lncRNAs play their roles by participating in epigenetic regulation, gene transcription, protein transport, cell proliferation, and differentiation.[6-9] The first lncRNA reported to be involved in tumor progression was HOX transcript antisense RNA (HOTAIR). In breast cancer, the enforced expression of HOTAIR interacts with polycomb repressive complex 2, leading to histone H3 lysine 27 methylation and thereby increasing breast cancer cell invasion and migration.[10] In GC, HOTAIR acts as a competing endogenous RNA to sink miR-331-3p, thereby inducing derepression of human epidermal growth factor receptor 2 to promote the proliferation, migration, and invasion of GC cells and predicting the poor prognosis of GC patients.[11] Subsequent studies have found that HOTAIR plays oncogenic roles in many malignant tumors, such as ovarian cancer,[12] cervical cancer,[13] liver cancer,[14] and colorectal cancer.[15]

Also known as ESE-1, ELF-3 is a subgroup of the epithelium-specific ETS transcription factors. Katey et al[16] reported that high ELF3 expression was associated with poor survival in the adenocarcinoma subtype of lung cancer but not in squamous cell lung cancer. Shinichi et al[17] identified ELF3 as a significantly mutated driver gene in ampullary carcinoma. The knockdown of ELF3 increased the invasive activity and motility and induced epithelial to mesenchymal transition (EMT) in immortalized normal epithelial cell lines but did not affect proliferation. We found two novel lncRNAs that were highly expressed in GC tissues in the Gene Expression Omnibus (GEO) database, one of which was our previously reported TMEM-AS1,[18] while the other was ELF3-AS1. The lncRNA ELF3-AS1, also known as SCAT7, is an ELF3 antisense RNA1. Several articles later reported that ELF3-AS1 plays oncogenic roles in bladder cancer,[19] non–small cell lung cancer (NSCLC),[20] glioma,[21] osteosarcoma,[22] and oral squamous cell cancer.[23] In this study, we investigated the effect of ELF3-AS1 on the function of GC cells and explored the precise mechanism of its effects.

2 | MATERIALS AND METHODS

2.1 | Tissue collection and ethics statement

A total of 103 GC patients who underwent surgery in Harbin Medical University Cancer Hospital between 2012 and 2014 were enrolled in this study. None of these patients received transfusion before blood test and neoadjuvant chemotherapy or radiotherapy before surgery. Clinical pathological data were collected from the medical records. All the tissues were sectioned immediately after being isolated, frozen in liquid nitrogen, and stored at −80°C. Patients were followed up every 3 months during the first 2 years after surgery and every 1 year after 2 years. The follow-up deadline was December 31, 2018. Overall survival (OS) was defined from the time of surgery to death, and disease-free survival (DFS) was defined from the time of surgery to disease recurrence or progression. This study was approved by the Medical Ethics Committee of the Harbin Medical University Cancer Hospital. All the patients signed informed consent to allow the use of their medical information for future studies.

2.2 | RNA extraction and quantitative reverse-transcriptase polymerase chain reaction (RT-qPCR) analyses

The RNA was extracted from tissues and cells using TRIzol reagent (Life Technologies). The total RNA was reverse-transcribed into cDNA using a reverse transcription kit (Takara). The quantitative RT-qPCR analyses were performed using SYBR Green (Takara). The results were normalized to glyceraldehyde-3-phosphate dehydrogenase (GAPDH). The primer sequences are listed in Table S1.

2.3 | Cell lines and reagents

The GC cell lines (BGC823, SGC7901, HGC27, AGS, MGC803, and MKN45) and the normal gastric mucosal epithelial cell line GES1 were purchased from the Cell Bank of Chinese Academy of Sciences (Shanghai, China). Cells were cultured in humidified atmosphere with 5% CO2 in DMEM or RPMI 1640 (GIBCO-BRL) and plus 10% fetal bovine serum (FBS; Invitrogen) and 100 U/mL penicillin and 100 mg/mL streptomycin.

2.4 | Transfection of cell lines

The ELF3-AS1 cDNA was synthesized and cloned into the expression vector pcDNA3.1 (Invitrogen). The ELF3-AS1 siRNAs were purchased from Santa Cruz Biotechnology. Lipofectamine2000 (Invitrogen) was used for the transfection of cells with the siRNA and plasmid. The negative controls were si-NC and empty vector pcDNA.

2.5 | Cell proliferation analysis

The MTT assays were used to assess cell viability. Colony formation assays were performed in which 1000 cells were seeded in each well of a six-well plate, and the medium containing 10% FBS was changed every 4 days. The cloned spots were fixed with methanol for 15 minutes, stained with 0.1% crystal violet for 20 minutes, and then counted. The 5-ethynyl-2'-deoxyuridine (EdU) proliferation assays were performed with an EdU Cell Proliferation Assay Kit (Ribobio, Cat. No. C10310) according to the manufacturer's instructions.

2.6 | Flow cytometry analysis

The cells were collected 48 hours after transfection. For cell cycle experiments, cells were fixed with propidium iodide, and the proportion of cells in G0/G1, S, and G2/M phases was measured using the CycleTESTTM PLUS DNA Kit (BD Biosciences). For the apoptosis experiments, the cells were treated with fluorescein isothiocyanate-annexin V and propidium iodide according to the manufacturer's instructions and then identified by FACScan as survival, death, early apoptosis, or late apoptosis.

2.7 | Transwell assays

After transfection, 20 000 cells in 1% FBS medium were placed in the top chamber (pore size 8 μm; Millipore), and medium containing 10% FBS was added to the bottom chamber. After 24 hours, the cells in the chamber were removed with a cotton swab, and the cells that migrated through the basement membrane of the chamber were fixed with methanol, stained with crystal violet, and counted.

2.8 | Western blot assay and antibodies

The cells were lysed with RIPA lysis buffer (Beyotime) containing protease inhibitors. Protein cleavage was separated by 10% SDS-PAGE electrophoresis, transferred to a 0.22 polyvinylidene fluoride membrane (Millipore), and incubated with specific antibodies. β-actin was used as an internal control. Anti-E-cadherin, anti-vimentin, anti-cyclin D1, and anti-P21 antibodies were purchased from Abcam. Anti-CDK6 antibodies were purchased from Cell Signaling Technology. Anti-MMP9, anti-MMP7, anti-CCL20, anti-THPO, and anti-CCR6 antibodies were purchased from Affinity Biosciences.

2.9 | In vivo assay

Four-week-old athymic male nude mice were purchased from the Animal Center of the Chinese Academy of Science and were bred under specific pathogen-free conditions. The BGC823 cells transfected with sh-ELF3-AS1 or sh-Ctrl using lentivirus (Genechem) were injected simultaneously into the nude mice. The tumor volumes were measured as length × width^2 × 0.5 and recorded every 2 days after the formation of visible tumors. Mice were sacrificed after 16 days, and the tumors were weighed and used for future studies.

2.10 | Subcellular fractionation location

The separation of the nuclear and cytosolic fractions was performed using the PARIS Kit (Life Technologies) according to the manufacturer's instructions.

2.11 | Transcriptome sequencing

The total RNA extracted from the BGC823 cells with ELF3-AS1 knockdown and control cells was quantified and assessed using the Agilent2200 system (Agilent). The sequencing library of each RNA sample was prepared using the Ion Proton Total RNA-Seq Kit v2 (Ambion). The data are available in Table S2.

2.12 | RNA immunoprecipitation assays

RNA immunoprecipitation (RIP) assays were performed with a Magna RIP™ RNA-binding protein immunoprecipitation kit (Millipore) following the manufacturer's instructions. Antibodies for RIP of hnRNPK, YBX1, VDR, KDM4A, DNMT1, LSD1, and BMI1 were purchased from Abcam.

2.13 | Chromatin immunoprecipitation assays

The chromatin immunoprecipitation (ChIP) assays were performed using the EZ-CHIP kit following the manufacturer's instructions (Cat. 17-408, Millipore). Immunoprecipitated DNA was quantified using qPCR. The ChIP data were calculated as percentages relative to the input DNA.

2.14 | Statistical analysis

All statistical analyses were performed using SPSS (version 17.0; IBM, SPSS). The comparisons between different groups were analyzed using count data in a Chi-square test. The comparison of OS and DFS was calculated using the Kaplan-Meier method with log-rank tests. The cutoff value for platelet to lymphocyte ratio (PLR) was determined by receiver operating curve (ROC) analysis. Variables with $P < .05$ in the univariate analysis were recruited into the multivariate Cox regression model with the backward likelihood ratio (LR) analysis to screen for independent risk factors that affect the prognosis. Student's *t*-test was used for the measurement data between the two groups, and a one-way ANOVA was used for the comparison of multiple groups (>2). The correlation between the expression of different genes was analyzed using Spearman's correlation test. Statistical significance was set at $P < .05$. All experiments were repeated at least in triplicate.

3 | RESULTS

3.1 | Expression and prognostic significance of ELF3-AS1 in GC

We analyzed GC data (GSE 51 308) from the GEO database and found that lncRNA ELF3-AS1 was upregulated in this group of GC tissues by lncRNA annotation (Figure 1A). We then analyzed the tissue data in this group and found that ELF3-AS1 was upregulated in three tissues (with an approximately 1.5-fold average increase), roughly the same in one tissue, and downregulated in the other tissues (Figure 1B). We then detected the expression level of ELF3-AS1 in the gastric mucosal epithelial cell line GES1 and GC cell lines (MGC803, BGC 823, SGC 7901, HGC 27, AGS, and MKN45). We found that ELF3-AS1 was highly expressed in the MKN45, AGS, BGC823, and SGC7901 cell lines, was downregulated in the MGC803 cell line, and there was no significant difference in HGC27 compared with GES1 (Figure 1C). These results suggest that ELF3-AS1 may be highly expressed in GC and may have potential cancer-promoting effects. We used RT-qPCR to detect the expression of ELF3-AS1 in 103 pairs of GC tissues and corresponding adjacent normal tissues. The results showed that ELF3-AS1 was expressed at low levels in 37 GC cases and high levels in 66 GC cases (Figure 1D).

Based on the expression level of ELF3-AS1, 103 patients were divided into a high-expression group (n = 51) and a low-expression group (n = 52). The relationships between the expression levels of ELF3-AS1 and various clinicopathological factors were analyzed. The results showed that the expression of ELF3-AS1 in GC tissues was significantly associated with gender ($P = .023$), TNM stage ($P = .031$), radical surgery ($P = .010$), and metastatic lymph node ratio (MLNR) ($P = .009$). Associations with age ($P = .624$), T ($P = .776$), N ($P = .772$), maximum tumor diameter ($P = .487$), carcino-embryonic antigen (CEA) ($P = .401$), and carbohydrate antigen (CA) 19-9 ($P = .094$) were not significant (Table 1).

Our previously published data confirmed that PLR can be used to assess the prognosis of patients with GC.[24] We calculated the PLR values in this group of patients and used the ROC curve to obtain the optimal cutoff value. The area under the curve was 0.684, and the critical value was 118.12 (Figure 1E). We then divided the patients into a PLR ≤118.12 group and a PLR >118.12 group. The univariate survival analysis showed that the 5-year OS rate was 63.4% in patients with PLR ≤118.12, and the average OS was 50.2 months. The 5-year OS rate was 35.5% for patients with a PLR >118.12, and the average OS was 37.8 months. The differences between groups were statistically significant (Figure 1F; log-rank $P = .005$). The mean DFS was 45.6 months in the PLR ≤118.12 group, while it was 35.6 months in the PLR >118.12 group. The differences were statistically significant (Figure 1F, log-rank, $P = .013$). In contrast, in the ELF3-AS1 low-expression group, the 5-year OS rate was 55.8% and the average OS was 50.2 months, while it was 37.3% and 35.6 months, respectively, in the high-expression group. The differences between groups were statistically significant (Figure 1G, log-rank, $P = .018$). The mean DFS was 47.4 months in the low-expression group and 33.2 months in the high-expression group, which was significantly different (Figure 1G, log rank, $P = .031$).

FIGURE 1 Expression of the long noncoding RNA (lncRNA) ELF3-AS1 in gastric cancer (GC) tissues and its effect on the prognosis of GC patients. A, The expression levels of different lncRNAs in tumor tissues and adjacent normal tissues in the Gene Expression Omnibus (GEO) database GSE51308 group. B, The expression of lncRNA ELF3-AS1 in five pairs of cancer and adjacent normal tissues in GSE51308. C, The expression levels of lncRNA ELF3-AS1 in different GC cell lines and normal gastric mucosal epithelial cells. ELF3-AS1 was more highly expressed in the MKN45, HGC27, BGC823, SGC7901, and AGS cell lines than the GSE-1 cell. D, The expression level of lncRNA ELF3-AS1 in 103 patients with GC was detected by quantitative reverse-transcriptase polymerase chain reaction; the expression level was high in 66 patients and low in 37 patients. E, Receiver operating curve based on the survival of GC patients was used to achieve the optimal cutoff value of the platelet to lymphocyte ratio (PLR). F, Differences in the overall survival time and progression-free survival time of GC patients with PLR ≥118.12 and PLR <118.12. G, The effect of the ELF3-AS1 expression level on the overall survival time and disease-free survival time of patients with GC; the overall survival time and disease-free survival time of patients with high ELF3-AS1 expression were worse than those of patients with low ELF3-AS1 expression

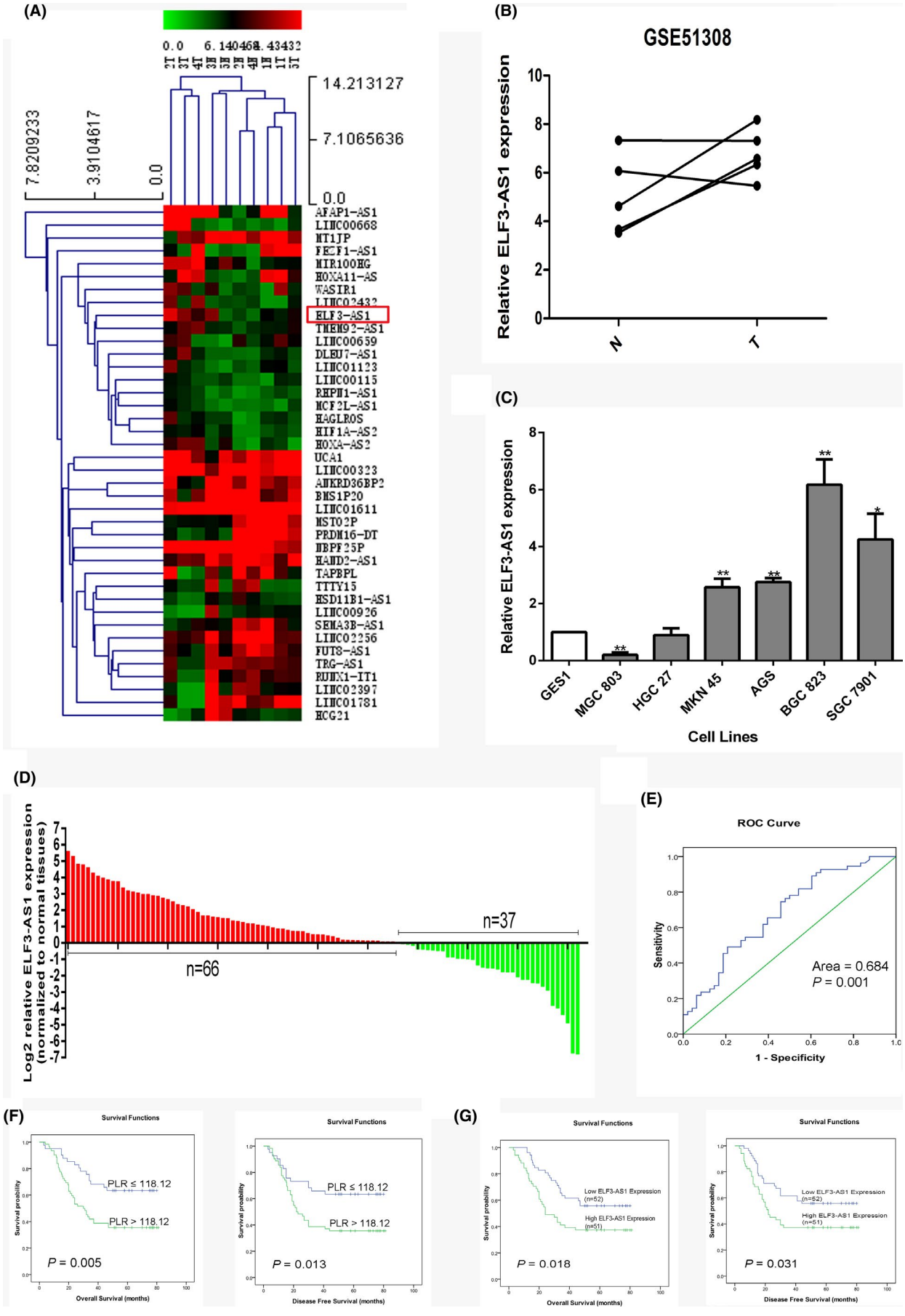
(A)
0.0
6.140468.43432
14.213127
7.1065636
0.0
7.8209233
3.9104617
0.0
AFAP1-AS1
LINC00668
MT1JP
FECF1-AS1
MIR100HG
HOXA11-AS
WASIR1
LINC02432
ELF3-AS1
TMEM92-AS1
LINC00659
DLEU7-AS1
LINC01123
LINC00115
RHPN1-AS1
MCF2L-AS1
HAGLROS
HIF1A-AS2
HOXA-AS2
UCA1
LINC00323
ANKRD36BP2
BMS1P20
LINC01611
MSTO2P
PRDM16-DT
MBPF25P
HAND2-AS1
TAPBPL
TTTY15
HSD11B1-AS1
LINC00926
SEMA3B-AS1
LINC02256
FUT8-AS1
TRG-AS1
RUNX1-IT1
LINC02397
LINC01781
HCG21
(B)
GSE51308
Relative ELF3-AS1 expression
N
T
(C)
Relative ELF3-AS1 expression
GES1
MGC 803
HGC 27
MKN 45
AGS
BGC 823
SGC 7901
Cell Lines
(D)
Log2 relative ELF3-AS1 expression (normalized to normal tissues)
n=66
n=37
(E)
ROC Curve
Sensitivity
1 - Specificity
Area = 0.684
P = 0.001
(F)
Survival Functions
PLR ≤ 118.12
PLR > 118.12
P = 0.005
Survival probability
Overall Survival (months)
Survival Functions
PLR ≤ 118.12
PLR > 118.12
P = 0.013
Survival probability
Disease Free Survival (months)
(G)
Survival Functions
Low ELF3-AS1 Expression (n=52)
High ELF3-AS1 Expression (n=51)
P = 0.018
Survival probability
Overall Survival (months)
Survival Functions
Low ELF3-AS1 Expression (n=52)
High ELF3-AS1 Expression (n=51)
P = 0.031
Survival probability
Disease Free Survival (months)

TABLE 1 Correlations between ELF3-AS1 and clinicopathological characteristics of gastric cancer (GC) patients

Variables	Low expression	High expression	χ^2	*P*-value
Gender				
Female	43	32	5.176	.023
Male	9	19		
Age(y)				
≤60	28	25	0.240	.624
>60	24	26		
T				
T1-2	6	5	0.081	.776
T3-4	46	46		
N				
N0	11	12	0.084	.772
N1-3	41	39		
TNM stages				
I, II	25	14	4.656	.031
III, IV	27	37		
Maximum diameter(cm)				
≤6.26	36	32	0.483	.487
>6.26	16	19		
Radicality				
R0	45	33	6.677	.010
R1, R2	7	18		
MLNR[a]				
≤23.98%	25	12	6.740	.009
>23.98%	27	39		
CEA				
≤5	45	41	0.706	.401
>5	7	10		
CA199				
≤37	47	40	2.804	.094
>37	5	11		

Abbreviation: MLNR, metastatic lymph node ratio.
[a]The average point of MLNR was 23.98%.

We then performed a survival analysis for OS. The univariate analysis showed that T ($P = .001$), N ($P < .001$), TNM stage ($P < .001$), radicality ($P < .001$), maximum tumor diameter ($P < .001$), MLNR ($P < .001$), PLR ($P = .013$), and ELF3-AS1 ($P = .031$) expression levels were associated with OS in patients with GC, while age ($P = .806$), sex ($P = .726$), CEA ($P = .131$), and CA19-9 ($P = .068$) were not associated with OS (Table 2). Factors significantly associated with OS in the univariate analysis were included in the Cox multivariate regression analysis, and the results showed that the TNM stage ($P < .001$), maximum tumor diameter ($P = .016$), and ELF3-AS1 expression level ($P = .016$) were regarded as independent risk factors affecting OS in patients with GC.

Finally, we performed a survival analysis on DFS. The univariate analysis showed that the T ($P = .001$), N ($P < .001$), TNM stage ($P < .001$), radicality ($P < .001$), maximum tumor diameter ($P = .001$), MLNR ($P < .001$), PLR values, and ELF3-AS1 expression levels were associated with DFS, while age ($P = .864$), sex ($P = .657$), CEA ($P = .111$), and CA19-9 ($P = .120$) were not (Table 3). Factors significantly affecting DFS in univariate analysis were included in the Cox multivariate regression analysis, and only MLNR ($P = .005$) and TNM stage ($P < .001$) were identified as independent risk factors for DFS, while the ELF3-AS1 expression level ($P = .086$) was not. Based on the above results, ELF3-AS1 was highly expressed in GC tissues and affected the prognosis of patients with GC.

3.2 | ELF3-AS1 promotes proliferation and migration of GC cells

As ELF3-AS1 had the highest expression levels in BGC823 and SGC7901, we selected these two cell lines for the cell function experiments. We designed three siRNA interference sequences to knockdown ELF3-AS1, and transfected si-ELF3-AS1 1#, 2#, and 3# in BGC823 and SGC7901 cells. The RNA extraction and RT-qPCR showed that si-ELF3-AS1 1# and 3# had higher interference efficiency, reaching more than 75% (Figure 2A). We chose si-ELF3-AS1 1# and 3# for subsequent functional testing.

The MTT assays showed that the knockdown of ELF3-AS1 significantly inhibited the proliferation of GC cells (Figure 2B). The colony formation assays demonstrated that the clonogenetic survival of GC cells was significantly inhibited by ELF3-AS1 knockdown in both the BGC823 and SGC7901 cell lines (Figure 2C). The results of the EdU assay showed that the knockdown of ELF3-AS1 significantly reduced the proportion of EdU-positive cells (Figure 2D). Flow cytometry was used to detect changes in the cell cycle and apoptotic cell ratio after the knockdown of ELF3-AS1. The results showed that the knockdown of ELF3-AS1 slightly but significantly increased the proportion of G0/G1 phase cells in the SGC7901 cells, but there was no significant change in the proportion of G0/G1 cells in the BGC823 cell line (Figure 2E). The knockdown of ELF3-AS1 significantly increased the proportion of apoptotic cells in the BGC823 and SGC7901 cells (Figure 2F). To detect the effect of ELF3-AS1 on GC cell migration, we performed the Transwell assays. The results showed that the knockdown of ELF3-AS1 significantly reduced the number of cells that sprawled through the basement membrane of the chamber (Figure 2G), indicating that the knockdown of ELF3-AS1 significantly inhibited the migration ability of the GC cells.

To better understand the effects of ELF3-AS1, we examined the changes in the function-related gene expression after the knockdown of ELF3-AS1. The RT-qPCR results showed that P21 and the epithelial marker E-cadherin were upregulated in both BGC823 and SGC7901 cell lines, while the mesenchymal marker vimentin and the

TABLE 2 Univariate and multivariate analysis of factors for overall survival (OS)

	Univariate analysis		Multivariate analysis	
Variables	***P***	**HR (95% CI)**	***P***	**HR (95% CI)**
Gender	.726	1.118 (0.600-2.083)		
Age	.806	0.936 (0.551-1.589)		
T	.001	2.191 (1.403-3.423)		
N	<.001	2.018 (1.607-2.535)	.057	1.339 (0.992-1.808)
TNM stages	<.001	6.180 (3.717-10.274)	<.001	4.129 (2.166-7.872)
Radicality	<.001	3.554 (2.037-6.200)		
Maximum diameter	<.001	2.740 (1.610-4.665)	.016	1.963 (1.136-3.461)
MLNR	<.001	7.321 (3.130-17.124)		
CEA	.131	1.638 (0.863-3.111)		
CA199	.068	1.817 (0.958-3.449)		
ELF3-AS1	.018	1.914 (1.118-3.275)	.016	1.974 (1.135-3.434)
PLR	.005	2.355 (1.298-4.272)		

Abbreviations: CI, confidence interval; HR, hazard ratio; MLNR, metastatic lymph node ratio; PLR, platelet to lymphocyte ratio.

matrix metalloproteinase family members MMP7 and MMP9 were downregulated (Figure 3A). The Western blot assays showed that the protein levels of MMP7, MMP9, and vimentin decreased after the knockdown of ELF3-AS1, while the expression of E-cadherin and P21 protein significantly increased. We then detected these changes in the other cell lines. After knocking down ELF3-AS1, similar trends of the above mRNAs and proteins were verified in the HGC27, MKN45, and AGS cell lines. However, with the overexpression of ELF3-AS1, we observed the opposite trends in the MGC803 cells (Figure S1).

3.3 | ELF3-AS1 promotes tumorigenic ability of GC cells in vivo

To detect the effect of ELF3-AS1 on the tumorigenic ability of GC cells, we transfected BGC823 cells with sh-Ctrl and sh-ELF3-AS1 to obtain monoclonal cells. We then established subcutaneous xenografts in the nude mice, and the size of subcutaneous xenografts of the two groups of mice were observed and recorded every 2 days after the formation of the tumors. The mice were sacrificed 2 weeks later, and the tumors were excised, photographed, and weighed. The results showed that the knockdown of ELF3-AS1 significantly inhibited the tumorigenic ability of the GC cells compared with the control group. The tumor weight and volume were significantly smaller than those in the control group (Figure 3D and E). The immunohistochemistry showed that the expression of Ki-67 in the sh-ELF3-AS1 group was significantly lower than that in the sh-Ctrl group (Figure 3F). To verify the effect of ELF3-AS1 knockdown on EMT in vivo, we also detected the EMT markers E-cadherin and vimentin. The results of the immunohistochemistry showed that the expression of E-cadherin was significantly increased, while that of vimentin was significantly decreased. Based on the above results, the ELF3-AS1 knockdown significantly inhibited the tumorigenic ability of the GC cells in vivo.

3.4 | Transcriptome sequencing to get downstream target genes of ELF3-AS1

To further investigate the mechanism by which ELF3-AS1 exerts its biological function, we examined the distribution of ELF3-AS1 in the BGC823 and SGC7901 cells using a nuclear separation assay. The results showed that ELF3-AS1 was distributed in both the nucleus and cytoplasm. The nucleoplasmic fraction was approximately half in the BGC823 cells, whereas it was much higher in the nucleus than in the cytoplasm in the SGC7901 cells (Figure 3C). Therefore, we hypothesized that ELF3-AS1 may play a role mainly at the transcriptional level. We examined the changes in the transcriptome mRNA after the knockdown of ELF3-AS1 in the BGC823 cells through high-throughput sequencing. The results showed that, compared with the control group, 2022 genes were upregulated, 2056 genes were downregulated, and 25 464 were undifferentiated genes (Figure 3G and H). To investigate the biological functions of the differentially expressed genes in the transcriptome sequencing results, we performed a functional enrichment analysis to achieve functional genomics annotations on the sequencing results. The results of the enrichment analysis showed that these genes were mainly involved in cell proliferation, adhesion, invasion, and metastasis (Figure 3I), and the results were consistent with the results of our cell function experiments. Next, we used RT-qPCR to validate the inflammation-related genes that were corrected for cell proliferation, invasion, and migration (Figure 4A).

The results showed that, in both BGC823 and SGC7901 cells, the mRNA levels of CCL5 and CCL20 were downregulated, while P27, RB1, and FBP1 were upregulated. Interleukin-6 (IL6), IL8, and CXCL3 were downregulated in the BGC823 cells and upregulated in the SGC7901 cells. Considering these results, CCL5, CCL20, P27, RB1 and, and FBP1 can be regarded as downstream target genes of ELF3-AS1.

3.5 | Identification of downstream target gene function of ELF3-AS1

It has been reported that the combination of CCL20 and CXCL8 can promote EMT in colorectal cancer cells, and CCL20 or CXCL8 alone or together can promote cell proliferation, invasion, and migration.[25] We selected CCL20 as a downstream target gene for ELF3-AS1, and Western blotting showed that CCL20 protein expression was also significantly reduced after the knockdown of ELF3-AS1 (Figure 4B). We designed si-CCL20 1#, 2# and 3# and verified the interference efficiencies of si-CCL20 2# and 3# by more than 80% in both the BGC823 and SGC7901 cells (Figure 4C). At the same time, we performed full-length sequencing of ELF3-AS1 in the BGC823 cells, designed the overexpression plasmid pcDNA-ELF3-AS1 based on the rapid amplification of cDNA ends (RACE) results, and confirmed the overexpression efficiency in both cell lines (Figure 4C).

We then used si-CCL20 3# and pcDNA-ELF3-AS1 for rescue experiments to verify the function of CCL20 in cell proliferation and its functional relationship with ELF3-AS1. The results of the MTT assays showed that cell proliferation was significantly inhibited by CCL20 knockdown, and ELF3-AS1 overexpression promoted cell proliferation, which was suppressed by CCL20 knockdown (Figure 4D). The colony formation assays showed that the downregulation of CCL20 reduced clonogenetic survival, and ELF3-AS1 overexpression reversed the clonogenetic survival that was inhibited by CCL20 knockdown (Figure 4E). In addition, just knocking down CCL20 using si-CCL20 2# and 3# also attenuated migration in BGC 823 and SGC 7901 cells, as measured by transwell and wound healing assays (Figure 4F and G).

We detected the mRNA and protein expression levels of MMP7, E-cadherin, vimentin, P21, and CCR6 (the receptor of CCL20) after CCL20 knockdown by si-CCL20 2# and 3# in the BGC823 and

TABLE 3 Univariate and multivariate analysis of factors for disease free survival (DFS)

	Univariate analysis		Multivariate analysis	
Variables	***P***	**HR (95% *CI*)**	***P***	**HR (95% *CI*)**
Gender	.657	1.151(0.618-2.145)		
Age	.864	0.955(0.562-1.621)		
T	.001	2.159(1.384-3.367)		
N	<.001	2.163(1.700-2.752)	.005	1.573 (1.149-2.153)
TNM stages	<.001	5.738(3.471-9.485)	<.001	3.414 (1.807-6.451)
Radicality	<.001	3.316(1.899-5.789)		
Maximum diameter	.001	2.486(1.461-4.228)		
MLNR	<.001	7.371(3.142-17.292)		
CEA	.111	1.685(0.886-3.201)		
CA199	.120	1.661(0.875-3.153)		
ELF3-AS1	.031	1.806(1.056-3.091)	.086	1.617(0.934-2.799)
PLR	.013	2.127(1.172-3.859)		

Abbreviations: CI, confidence interval; HR, hazard ratio; MLNR, metastatic lymph node ratio; PLR, platelet to lymphocyte ratio.

FIGURE 2 Long noncoding RNA (lncRNA) ELF3-AS1 promoted the proliferation and migration of gastric cancer (GC) cells in vitro. A, The interference efficiency of three interference sequences in the BGC823 and SGC7901 cell lines was detected; the interference efficiency of si-ELF3-AS1 1# and 3# was higher than that of si-ELF3-AS1 2#. B, The MTT assay was used to detect the effect of the knockdown of ELF3-AS1 on the proliferation of GC cells in the BGC823 and SGC7901 cells. C, The clonal formation assay was used to detect the effect of the knockdown of ELF3-AS1 on the clonal formation ability of GC cells in the BGC823 and SGC7901 cells. D, The 5-ethynyl-2'-deoxyuridine (EdU assay was used to detect the effect of the knockdown of ELF3-AS1 on the proliferation of GC cells. E, Flow cytometry was used to detect the effect of the knockdown of ELF3-AS1 on the cell cycle of BGC823 and SGC7901. F, The flow cytometry apoptosis assay was used to detect the changes in the proportion of apoptotic cells after the knockdown of ELF3-AS1. G, The Transwell assay was used to detect the effect of the knockdown of ELF3-AS1 on the migration ability of GC cells

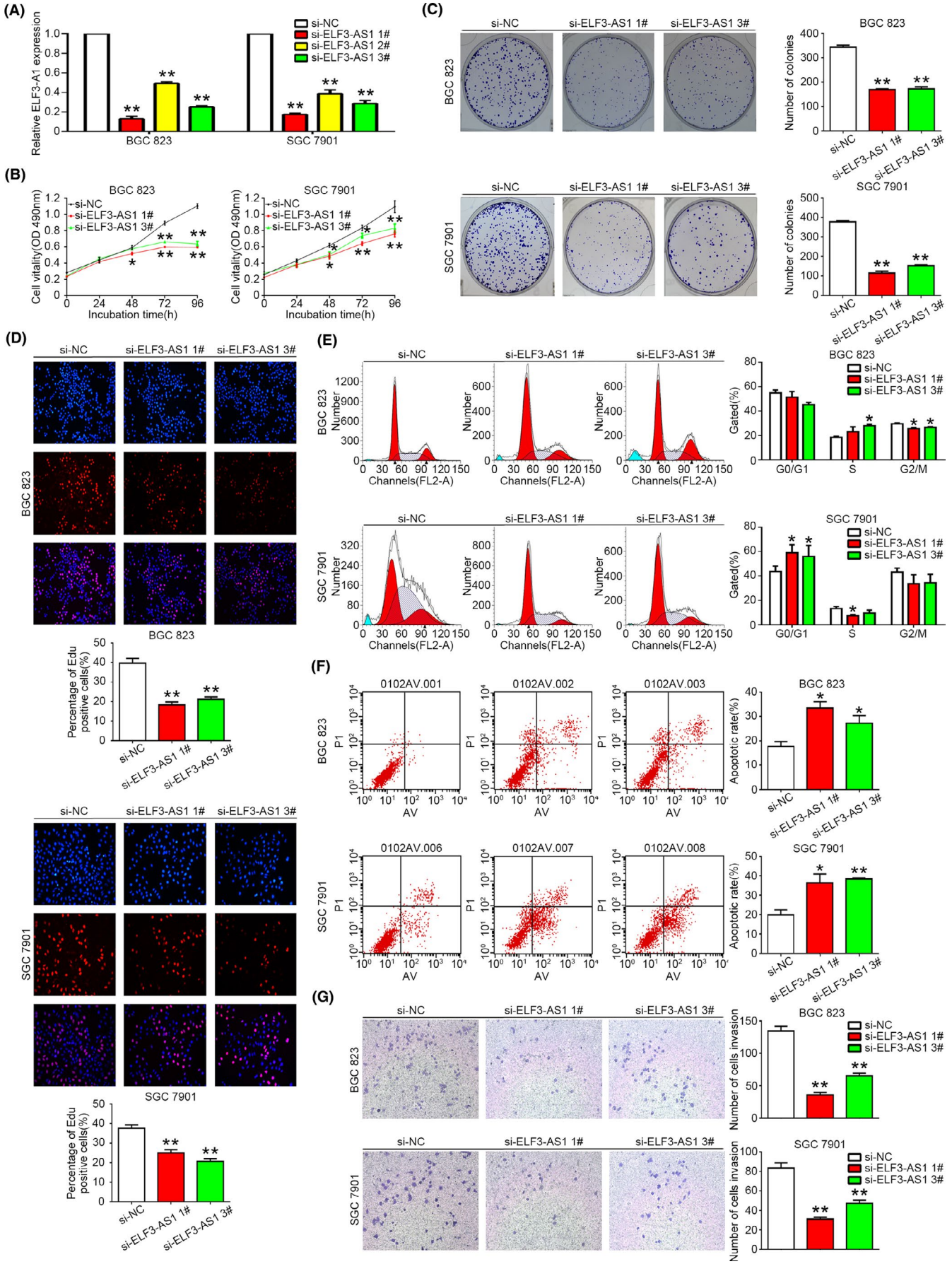
(A)
Relative ELF3-A1 expression
si-NC
si-ELF3-AS1 1#
si-ELF3-AS1 2#
si-ELF3-AS1 3#
BGC 823
SGC 7901
(B)
BGC 823
SGC 7901
Cell vitality(OD 490nm)
Incubation time(h)
(C)
si-NC
si-ELF3-AS1 1#
si-ELF3-AS1 3#
BGC 823
SGC 7901
Number of colonies
(D)
BGC 823
SGC 7901
Percentage of Edu positive cells(%)
(E)
Number
Channels(FL2-A)
Gated(%)
G0/G1
S
G2/M
(F)
0102AV.001
0102AV.002
0102AV.003
0102AV.006
0102AV.007
0102AV.008
P1
AV
Apoptotic rate(%)
(G)
Number of cells invasion

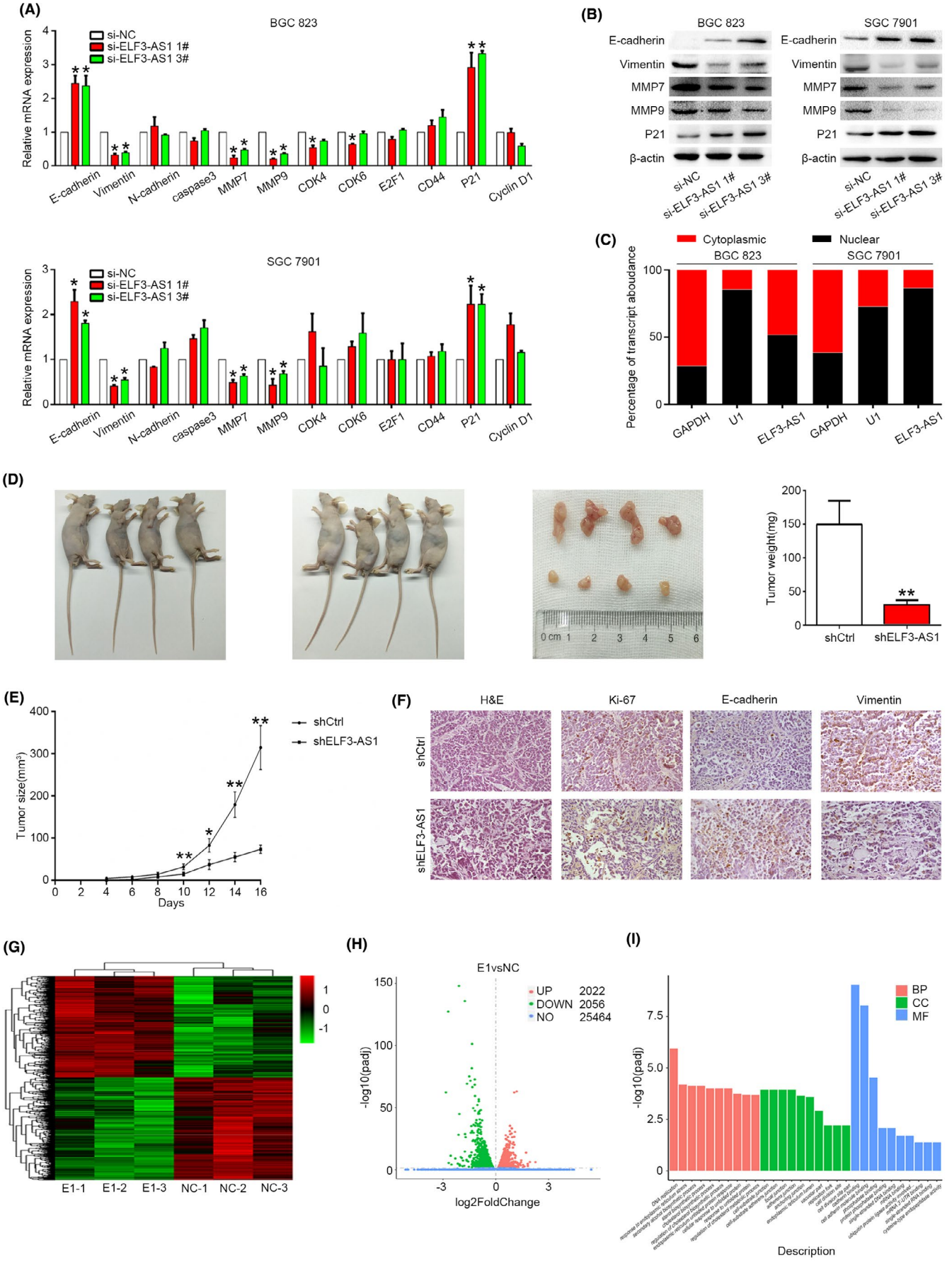
(A)
BGC 823
si-NC
si-ELF3-AS1 1#
si-ELF3-AS1 3#
Relative mRNA expression
E-cadherin
Vimentin
N-cadherin
caspase3
MMP7
MMP9
CDK4
CDK6
E2F1
CD44
P21
Cyclin D1
SGC 7901
(B)
BGC 823
SGC 7901
E-cadherin
Vimentin
MMP7
MMP9
P21
β-actin
si-NC
si-ELF3-AS1 1#
si-ELF3-AS1 3#
(C)
Cytoplasmic
Nuclear
Percentage of transcript aboudance
GAPDH
U1
ELF3-AS1
(D)
Tumor weight(mg)
shCtrl
shELF3-AS1
(E)
Tumor size(mm³)
Days
(F)
H&E
Ki-67
E-cadherin
Vimentin
(G)
E1-1
E1-2
E1-3
NC-1
NC-2
NC-3
(H)
E1vsNC
UP 2022
DOWN 2056
NO 25464
-log10(padj)
log2FoldChange
(I)
BP
CC
MF
Description

FIGURE 3 Effect of the long noncoding RNA (lncRNA) ELF3-AS1 on subcutaneous tumorigenic ability in nude mice and its effect on cell functional gene expression. Knockdown effects of ELF3-AS1 on the mRNA (A) and protein expression (B) levels of certain functional genes. C, After nuclear and cytoplasmic separation, RNA expression levels were measured. Glyceraldehyde-3-phosphate dehydrogenase (GAPDH) was used as a nuclear marker and U1 was used as a cytoplasmic marker. D, E, Effect of lentivirus knockdown of ELF3-AS1 expression on subcutaneous tumorigenic ability of GC cells in nude mice. F, Histopathological examination of subcutaneous tumors in sh-ELF3-AS1 and shCtrl groups; immunohistochemistry was used to detect the expression of Ki-67, E-cadherin, and vimentin. G, Comparison of transcriptome sequencing gene changes in the BGC823 cells with si-ELF3-AS1 1# knockdown ELF3-AS1 (differential multiples more than 2-fold). H, The number of post-variation genes after the knockdown of ELF3-AS1. I, The number of differential genes in biological processes, cellular components, and molecular functions

SGC7901 cells. The RT-qPCR results showed that the mRNA levels of MMP7, vimentin, and CCR6 significantly decreased after the knockdown of CCL20, while E-cadherin and P21 significantly increased (Figure 4H). The results of Western blotting were consistent with the RT-qPCR results (Figure 4I).

3.6 | ELF3-AS1 interacts with heterogeneous nuclear ribonucleoprotein K (hnRNPK) to regulate CCL20

Heterogeneous nuclear ribonucleoproteins (hnRNPs) are a large family of RNA-binding proteins (RBPs) that play important roles in nucleic acid metabolism.[26] One of the most extensively researched RBPs in the hnRNPs is hnRNPK, which is reportedly involved in erythrocyte differentiation, organ development, and tumorigenesis.[27,28] It is located both in the nucleus and cytoplasm and is capable of preferentially recognizing the ply-C sequence of the target gene through its three repetitive homologous domains (KH1, KH2, and KH3) and binding to the 3'UTR of the target mRNA, which encodes the proteins that participate in the regulation of cell proliferation, differentiation, and apoptosis.[29,30] Recently, numerous studies have reported that lncRNAs binding to hnRNPK regulate gene expression, participate in DNA damage, and promote tumorigenesis.[31,32] Other RBPs such as YBX1,[33] KDM4A,[34] and ESR1[35] have been extensively studied and were verified to interact with lncRNAs. To search for the appropriate RBP that interacts with ELF3-AS1, we performed RIP assays in the BGC823 cells using hnRNPK, YBX1, KDM4A, and ESR1 antibodies. The results showed that ELF3-AS1 bound to the hnRNPK protein with the highest abundance (Figure 5A). We then compared changes in the hnRNPK levels after ELF3-AS1 knockdown and found that ELF3-AS1 knockdown did not change the hnRNPK mRNA and protein levels (Figures 4B and 5B). Subsequently, we examined the levels of CCL20 and hnRNPK after hnRNPK knockdown. The mRNA levels of hnRNPK and CCL20 significantly decreased, and the same results were verified by Western blotting (Figure 5C–E). Simultaneously, we examined the effect of hnRNPK on cell proliferation using the MTT and colony formation assays. The results showed that cell proliferation was significantly inhibited, and the number of clones was significantly reduced after hnRNPK knockdown (Figure 5F and G).

To verify the effect of ELF3-AS1 on the binding abundance of hnRNPK and CCL20, we performed ChIP assays with the ELF3-AS1 knockdown. The Chip-qPCR and electrophoresis results showed that the binding abundance of hnRNPK to the CCL20 promoter region was significantly reduced with ELF3-AS1 knockdown (Figure 5H). The qPCR and Western blot results showed that the expression level of CCL20 significantly increased when ELF3-AS1 was overexpressed, and overexpressed ELF3-AS1 could upregulate the reduced CCL20 caused by hnRNPK knockdown (Figure 5I). This suggests that CCL20 may be a common downstream target gene for hnRNPK and ELF3-AS1. We detected the correlation of ELF3-AS1, hnRNPK, and CCL20 expression levels in 30 GC tissues by qPCR. The results indicated that the expression of ELF3-AS1, hnRNPK, and CCL20 in the GC tissues was positively correlated (Figure 5J). This suggested that ELF3-AS1 exerted its function, at least partly, by binding with hnRNPK to regulate the expression of CCL20.

3.7 | ELF3-AS1 affects the inflammatory response and immune microenvironment

Numerous studies have reported that the antitumor inflammatory response has an important influence on the occurrence and progression of tumors. The inflammatory response can induce DNA damage and promote neovascularization, promote tumor growth, and tumor metastasis.[36-38] Our published results also demonstrated that inflammatory markers such as dNLR, MLR, and FMR were independent risk factors for the prognosis of patients with GC.[24,39] To this end, we collected and statistically analyzed the relationships between the expression levels of ELF3-AS1 and white cells, neutrophils, lymphocytes, monocytes, platelets, and fibrinogen and calculated PLR. The results showed that the PLR value and platelet count in the ELF3-AS1 high-expression group were significantly higher than those in the ELF3-AS1 low-expression group (Figure 6A).

Stone found that epithelial ovarian cancer can produce thrombopoietin (THPO), which leads to thrombocytosis in the peripheral blood, and platelets can promote tumor cell proliferation and change the tumor immunomicroenvironment.[40] Given the correlation between ELF3-AS1 expression levels and the platelet counts and PLR values found in our study, we hypothesized that ELF3-AS1 may exert its effects through THPO. We detected the

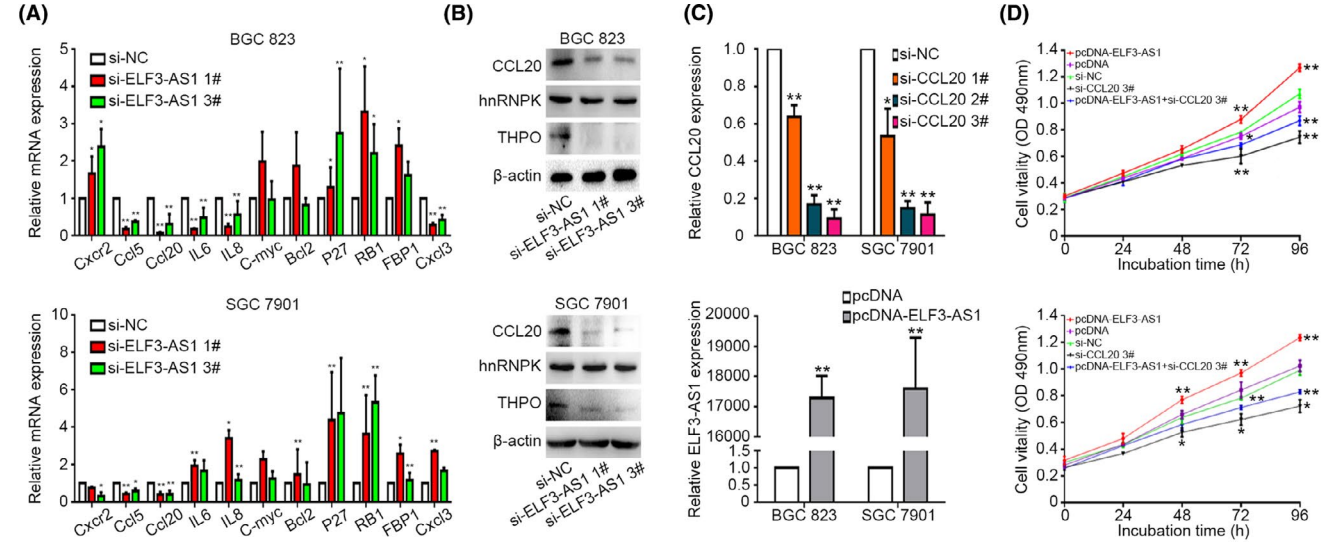
(A)
BGC 823
si-NC
si-ELF3-AS1 1#
si-ELF3-AS1 3#
Relative mRNA expression
Cxcr2 Ccl5 Ccl20 IL6 IL8 C-myc Bcl2 P27 RB1 FBP1 Cxcl3
SGC 7901
(B)
BGC 823
CCL20
hnRNPK
THPO
β-actin
si-NC
si-ELF3-AS1 1#
si-ELF3-AS1 3#
SGC 7901
(C)
Relative CCL20 expression
si-NC
si-CCL20 1#
si-CCL20 2#
si-CCL20 3#
BGC 823 SGC 7901
pcDNA
pcDNA-ELF3-AS1
Relative ELF3-AS1 expression
(D)
pcDNA-ELF3-AS1
pcDNA
si-NC
si-CCL20 3#
pcDNA-ELF3-AS1+si-CCL20 3#
Cell vitality (OD 490nm)
Incubation time (h)

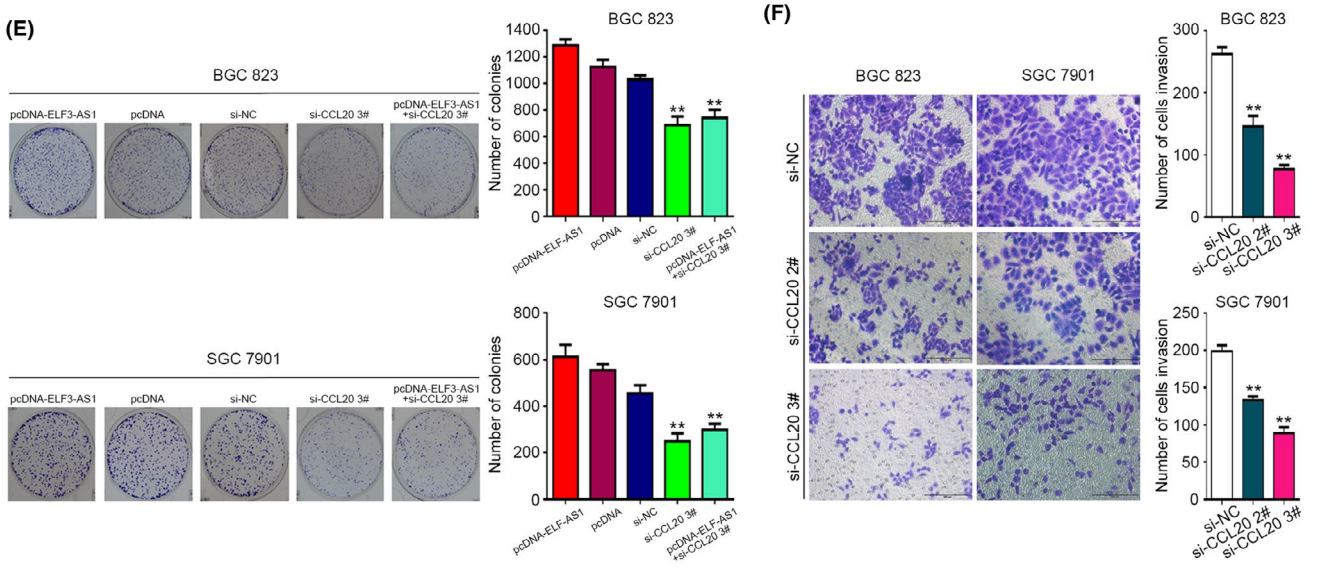
(E)
BGC 823
pcDNA-ELF3-AS1
pcDNA
si-NC
si-CCL20 3#
pcDNA-ELF3-AS1 +si-CCL20 3#
Number of colonies
SGC 7901
(F)
BGC 823
SGC 7901
si-NC
si-CCL20 2#
si-CCL20 3#
Number of cells invasion

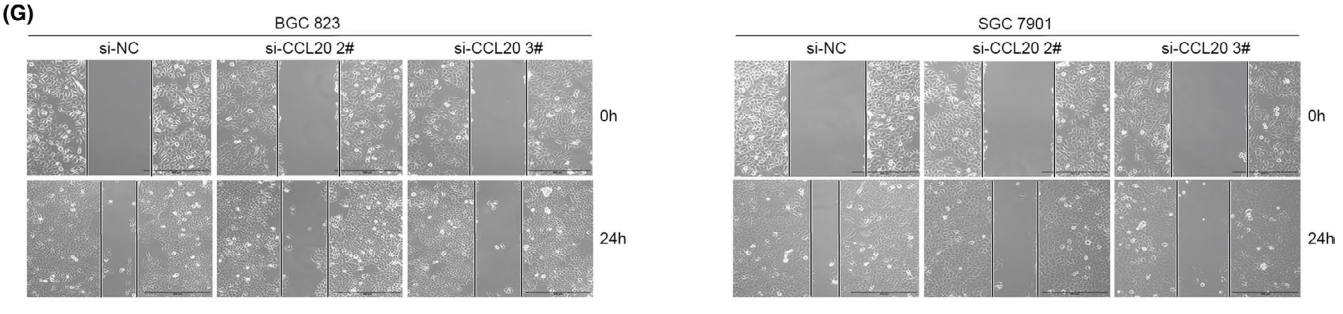
(G)
BGC 823
SGC 7901
si-NC
si-CCL20 2#
si-CCL20 3#
0h
24h

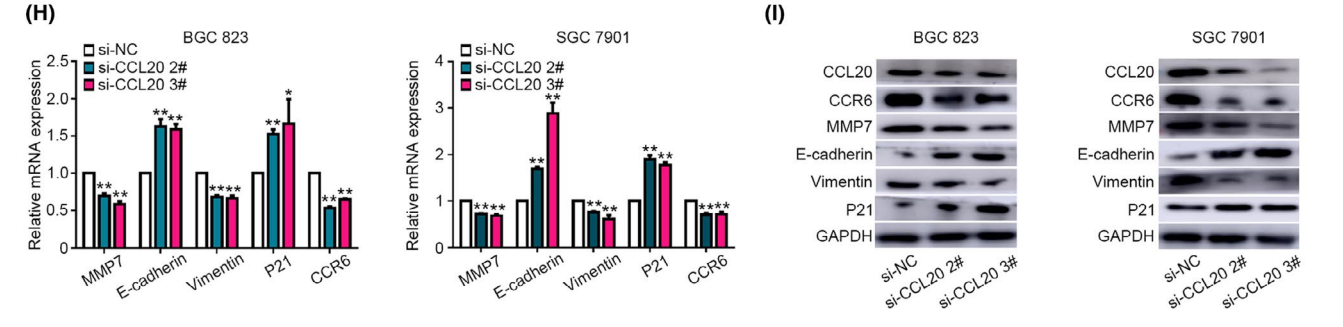
(H)
BGC 823
SGC 7901
si-NC
si-CCL20 2#
si-CCL20 3#
Relative mRNA expression
MMP7 E-cadherin Vimentin P21 CCR6
(I)
BGC 823
SGC 7901
CCL20
CCR6
MMP7
E-cadherin
Vimentin
P21
GAPDH
si-NC
si-CCL20 2#
si-CCL20 3#

FIGURE 4 Functional verification of the target gene downstream of ELF3-AS1. Partially differentially expressed functional genes were verified by (A) quantitative reverse-transcriptase polymerase chain reaction (RT-qPCR) and (B) Western blot in the BGC823 and SGC7901 cell lines. C, The qPCR verified the interference efficiency and overexpression efficiency of si-CCL20 and pcDNA-ELF3-AS1 in the BGC823 and SGC7901 cell lines. D, The MTT assay verified the effect of overexpression of ELF3-AS1 and knockdown of CCL20 on the proliferation of gastric cancer (GC) cells. E, Colony formation assays to verify the effect of the knockdown of CCL20 and overexpression of ELF3-A1 on the colony formation ability of GC cells. F, G, Transwell assay to verify the effect of CCL20 knockdown on the migration of GC cells. The qPCR (H) and Western blot (I) experiments to verify the expression of some functional genes regulated by ELF3-AS1 after the knockdown of CCL20

expression of THPO mRNA in the BGC823 and SGC7901 cells after ELF3-AS1 knockdown and found that THPO was significantly decreased (Figure 6B). Then, we examined THPO protein levels in the BGC823 and SGC7901 cells by Western blotting. The results showed that with ELF3-AS1 knockdown, the protein level of THPO was also significantly reduced (Figure 4B). The hnRNPK knockdown decreased the mRNA and protein levels of THPO (Figure 6B and Figure 5E). Overexpression of ELF3-AS1 promoted the expression of THPO, and overexpression of ELF3-AS1 partially reversed the inhibition of THPO expression by hnRNPK knockdown (Figure 6B and Figure 5I). Subsequently, we detected the expression of ELF3-AS1, hnRNPK, and THPO in 30 GC tissues. The results showed that the expressions of ELF3-AS1, hnRNPK, and THPO in the GC tissues were positively correlated (Figure 6C). We attempted to explore the correlation between the level of ELF3-AS1 in the tissues and the protein level of THPO in the peripheral blood but failed to uncover anything because of the extremely low level of THPO.

4 | DISCUSSION

Recently, a large number of studies have reported the relationships between the expression levels of lncRNAs and the prognosis of cancer patients and revealed the mechanism of their influence on tumor progression at the cellular level.[41,42] In the current study, we screened the lncRNA ELF3-AS1 from the database, which affected the prognosis of GC patients and promoted the proliferation and migration of GC cells. Our results demonstrated, for the first time, the role of ELF3-AS1 as an oncogene in promoting GC progression.

In recent years, a large number of tumor biological biomarkers have been discovered, some of which can be used to assess the prognosis of patients or detect tumors, such as the inflammation indicators NLR, multifactor integrated prediction model, and lncRNAs. The lncRNAs have different expression levels in different tissues and body fluids, and aberrantly expressed lncRNAs help identify the occurrence of disease, tumor staging, and the presence or absence of tumor recurrence and metastasis. For example, compared with prostate benign tumors, the prostate-specific lncRNA PCA3 is highly expressed in most prostate cancer patients, and high expression of PCA3 can be detected in urine, which is more convenient and noninvasive than measuring prostate-specific antigen in the peripheral blood.[43] In this study, we validated the effects of highly expressed ELF3-AS1 in GC tissues and cells and found that ELF3-AS1 is a biological marker for GC screening and assessing patient prognosis.

In our study, we found that higher ELF3-AS1 expression was associated with female sex, advanced stage, nonradical surgery, higher MLNR, and poor prognosis in GC patients and promoted GC cell proliferation and migration, inhibited apoptosis, and promoted the growth of transplanted tumors. These results indicate that ELF3 plays an oncogenic cancer-promoting role in GC. Although our current results showed that there were more women patients with higher ELF3-AS1 expression, we do not think that women were more likely to express higher ELF3-AS1 and have a worse prognosis. This may be because we collected fewer tissue samples, which were affected by the absolute number. In NSCLC and glioma studies reported in the literature, the expression of ELF3-AS1 did not differ between the sexes.[20,21] We plan to collect more samples to clarify this issue. Guo reported that ELF3-AS1 could promote bladder cancer cell viability, migration, and xenograft tumor growth, and research into the mechanism showed that ELF3-AS1 can interact with KLF8 to increase MMP9 expression.[19] Coincidentally, we also found that ELF3-AS1 promoted the expression of MMP9 and promoted EMT in GC cells. Meanwhile, a mechanistic study found that ELF3-AS1 may play a role in promoting cancer by binding hnRNPK to promote the expression of CCL20. CCL20 was reported to induce proliferation, migration, and invasion in colorectal cancer,[25] breast cancer,[44] thyroid cancer,[45] and hepatocellular carcinoma[46] by activating the PI3K/AKT-ERK1/2 pathway and NF-κB; increasing MMP2, MMP3, and MMP9 expression; and facilitating T_{reg} activity. In our study, we also found that CCL20 promoted proliferation and clonogenetic survival, increased MMP7 expression, and induced EMT in GC cells. These results were consistent with the results of the above studies, which also indicates that ELF3-AS1 functions by regulating CCL20 to some extent. The RBP hnRNPK plays a key role in linking ELF3-AS1 and CCL20.

Thrombocytosis has been reported in several cancers, including cervical cancer,[47] ovarian cancer,[48] colorectal cancer,[49] and GC.[39] Experimental evidence has shown that platelets promote tumors through a variety of mechanisms, including protecting tumor cells from immune cell surveillance, assisting tumor cells in new vasculature implantation, and promoting tumor angiogenesis.[50] However, the mechanism by which tumors induce thrombocytosis remains a mystery. Stone reported that excessive tumor-derived IL6 induced high expression of hepatic THPO synthesis, which led to paraneoplastic thrombocytosis.[33] In our study, we found that high ELF3-AS1 expression was associated with thrombocytosis, and IL6 and THPO

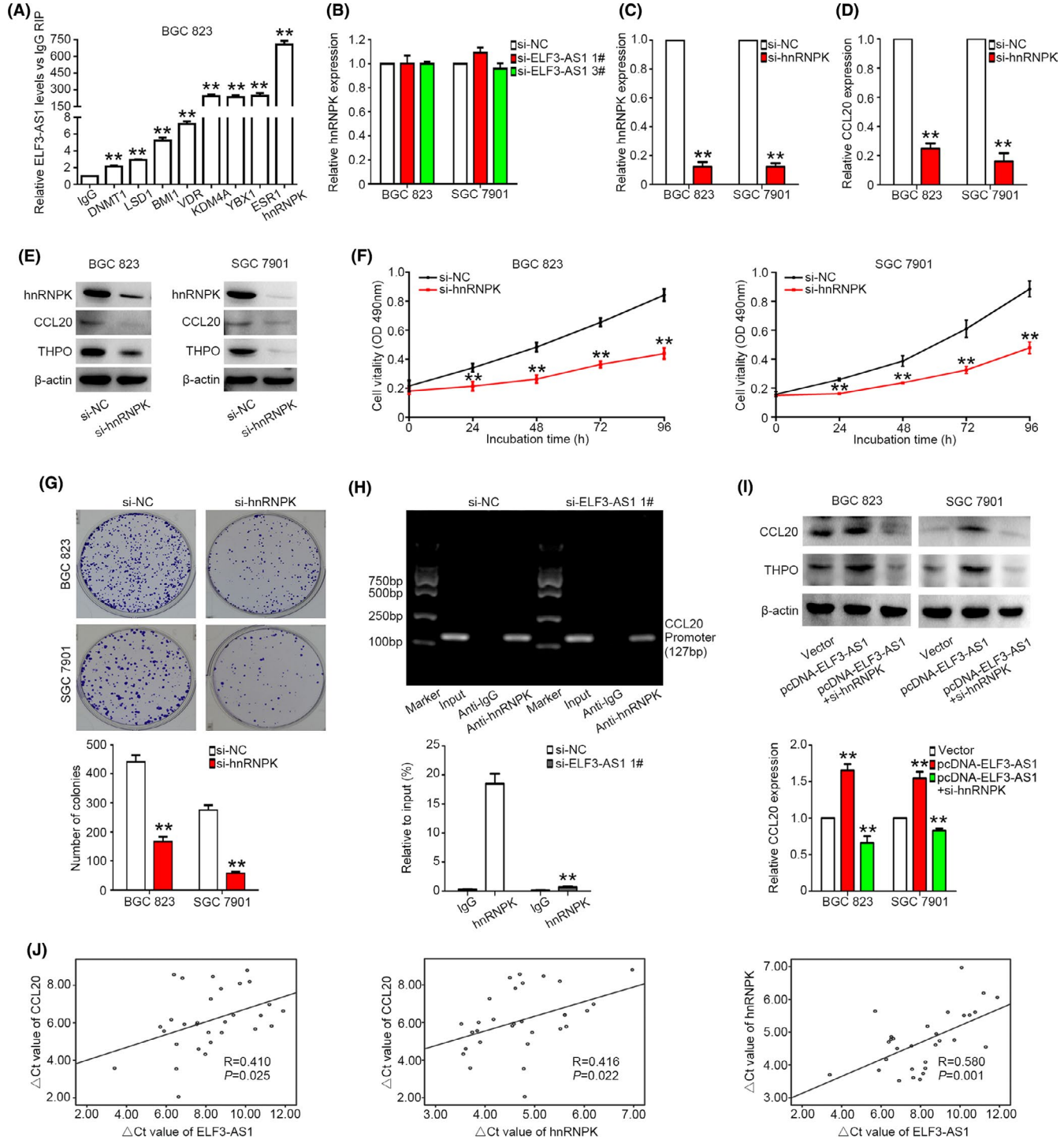

FIGURE 5 RNA immunoprecipitation (RIP) and chromatin immunoprecipitation (ChIP) experiments verify the role of ELF3-AS1 in regulating the downstream target gene CCL20. A, RIP assay to detect the binding abundance of ELF3-AS1 and related RNA-binding proteins. B, Quantitative polymerase chain reaction (qPCR) to verify the expression level of hnRNPK after the knockdown of ELF3-AS1. C, The interference efficiency of si-hnRNPK in the BGC823 and SGC7901 cell lines. The qPCR (D) and Western blot (E) experiments to verify the effect of the knockdown of hnRNPK on CCL20 and THPO expression. The MTT (F) and colony formation (G) assays to verify the effect of hnRNPK on cell proliferation. H, ChIP-qPCR detection of the knockdown of ELF3-AS1 on the binding abundance of hnRNPK and CCL20 promoter region, with IgG antibody as a negative control. I, The qPCR and Western blot experiments verify the effect of overexpression of ELF3-AS1 and the knockdown of hnRNPK simultaneously on the expression of the downstream target gene CCL20. J, The levels of ELF3-AS1, hnRNPK, and CCL20 in gastric cancer tissues were positively correlated

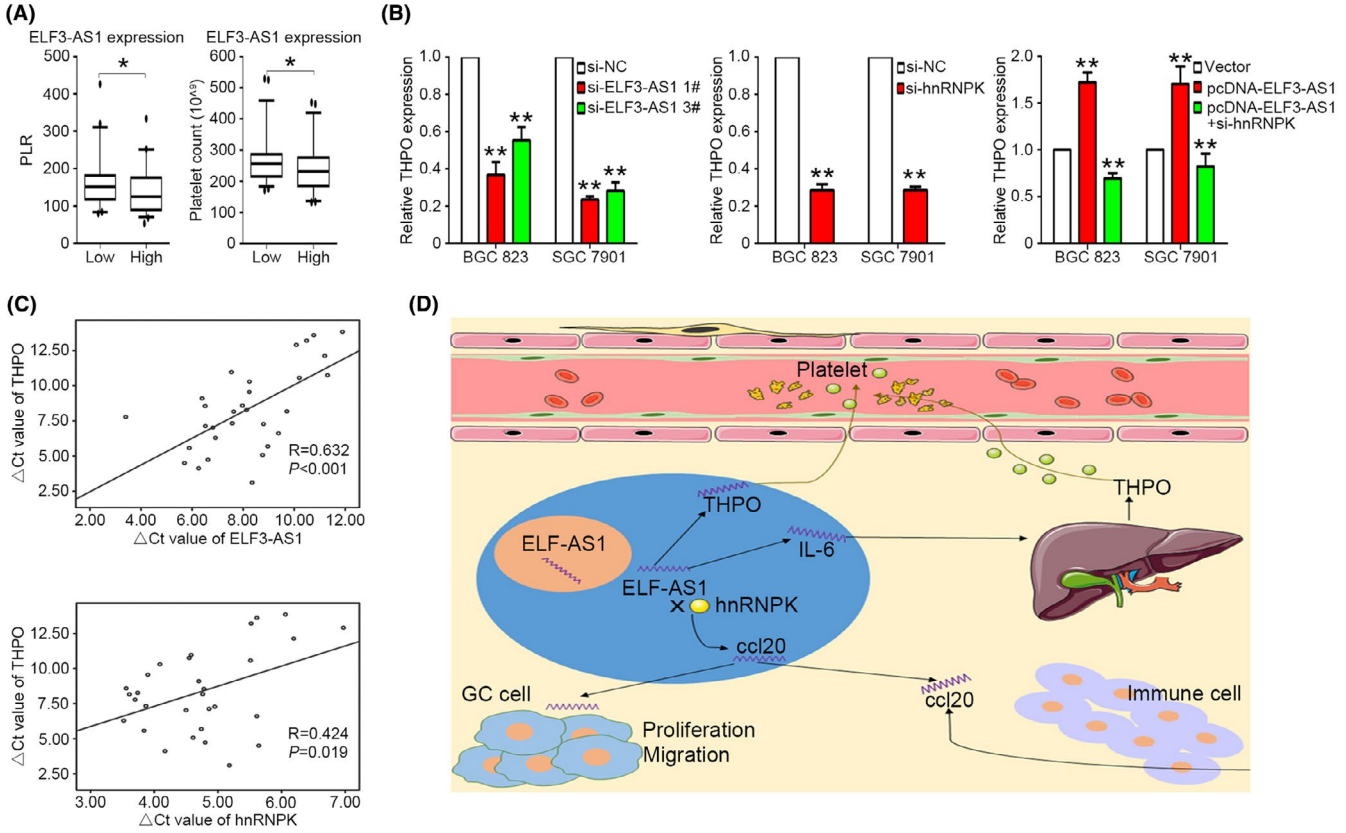

FIGURE 6 ELF3-AS1 regulates thrombopoietin (THPO) expression in gastric cancer (GC) cells. A, Comparison of blood platelet count and platelet to lymphocyte ratio (PLR) values in patients with high expression and low expression of ELF3-AS1. B, Expression levels of THPO after the knockdown of ELF3-AS1 and hnRNPK, and the overexpression of ELF3-AS1 and knockdown of hnRNPK, simultaneously. C, Quantitative polymerase chain reaction to verify the levels of ELF3-AS1, hnRNPK, and THPO in GC tissues. D, Hypothetical model of ELF3-AS1 in regulating the proliferation of GC cells and thrombocytosis in peripheral blood

were potential downstream target genes for ELF3-AS1. Although several studies have reported that tumor tissues and cells can produce THPO,[51,52] and we failed to verify the positive correlation between THPO and platelet count in the peripheral blood of GC patients, our research indicates the possibility that the high expression ELF3-AS1 in GC tissues promotes the expression and release of IL-6 into the blood and stimulates the liver to produce more THPO, or that GC tissues directly produce more THPO, resulting in an increase in blood platelet count. Verification of this hypothesis requires more research.

In conclusion, our current study demonstrated that the highly expressed lncRNA ELF3-AS1 predicted poor prognosis in GC patients and promoted the proliferation and migration of GC cells, which may be achieved by binding with hnRNPK to regulate the downstream target gene CCL20. Moreover, ELF3-AS1 can affect the immune microenvironment of GC, especially the platelet count, and the specific mechanism of this requires further research (Figure 6D).

ACKNOWLEDGMENT

Work on this article was supported by (1) the Harbin Science and Technology Bureau Research and Development Project of Applied Technology (2017RAXXJ054) and the Nn10 program of the Harbin Medical University Cancer Hospital (Nn 10PY2017-03); (2) the Grants from the Natural Science Foundation of Shandong Province (ZR2019MH109); and (3) the Grants from the National Natural Science Foundation of China (81730066 to D.M).

CONFLICT OF INTEREST

The authors declare no conflict of interest.

ORCID

Shubin Song https://orcid.org/0000-0002-6701-9668

REFERENCES

1. Bonelli P, Borrelli A, Tuccillo F, Silvestro L, Palaia R, Buonaguro F. Precision medicine in gastric cancer. *World Journal of Gastrointestinal Oncology*. 2019;11(10):804–829.
2. Amaral PP, Dinger ME, Mercer TR, Mattick JS. The eukaryotic genome as an RNA machine. *Science*. 2008;319(5871):1787-1789.
3. Guttman M, Amit I, Garber M, et al. Chromatin signature reveals over a thousand highly conserved large non-coding RNAs in mammals. *Nature*. 2009;458(7235):223-227.
4. Tzankov A, Gschwendtner A, Augustin F, et al. Diffuse large B-cell lymphoma with overexpression of cyclin e substantiates poor standard treatment response and inferior outcome. *Clin Cancer Res*. 2006;12(7 Pt 1):2125-2132.

5. Derrien T, Johnson R, Bussotti G, et al. The GENCODE v7 catalog of human long noncoding RNAs: analysis of their gene structure, evolution, and expression. *Genome Res*. 2012;22(9):1775-1789.
6. Lee JT. Epigenetic regulation by long noncoding RNAs. *Science*. 2012;338:1435-1439.
7. Ouyang J, Zhu X, Chen Y, et al. NRAV, a long noncoding RNA, modulates antiviral responses through suppression of interferon-stimulated gene transcription. *Cell Host Microbe*. 2014;16:616-626.
8. Lu Q, Ren S, Lu M, et al. Computational prediction of associations between long noncoding RNAs and proteins. *BMC Genom*. 2013;14:651.
9. Fatica A, Bozzoni I. Long non-coding RNAs: new players in cell differentiation and development. *Nat Rev Genet*. 2014;15:7-21.
10. Gupta RA, Shah N, Wang KC, et al. Long non-coding RNA HOTAIR reprograms chromatin state to promote cancer metastasis. *Nature*. 2010;464(7291):1071-1076.
11. Liu X, Sun M, Nie F, et al. Lnc RNA HOTAIR functions as a competing endogenous RNA to regulate HER2 expression by sponging miR-331-3p in gastric cancer. *Mol Cancer*. 2014;13(1):92.
12. Wang J, Chen D, He X, et al. Downregulated lincRNA HOTAIR expression in ovarian cancer stem cells decreases its tumorgeniesis and metastasis by inhibiting epithelial-mesenchymal transition. *Cancer Cell Int*. 2015;15(1):24.
13. Liu M, Jia J, Wang X, Liu Y, Wang C, Fan R. Long non-coding RNA HOTAIR promotes cervical cancer progression through regulating BCL2 via targeting miR-143-3p. *Cancer Biol Ther*. 2018;19(5):1-9.
14. Li H, An J, Wu M, et al. LncRNA HOTAIR promotes human liver cancer stem cell malignant growth through downregulation of SETD2. *Oncotarget*. 2015;6(29):27847-27864.
15. Dou J, Ni Y, He X, et al. Decreasing lncRNA HOTAIR expression inhibits human colorectal cancer stem cells.[J]. *Am J Transl Res*. 2016;8(1):98-108.
16. Enfield KSS, Marshall EA, Anderson C, et al. Epithelial tumor suppressor ELF3 is a lineage-specific amplified oncogene in lung adenocarcinoma. *Nat Commun*. 2019;10(1):5438.
17. Yachida S, Wood LD, Suzuki M, et al. Genomic Sequencing Identifies ELF3 as a Driver of Ampullary Carcinoma. *Cancer Cell*. 2016;29(2):229-240.
18. Song S, He X, Wang J, et al. A novel long noncoding RNA, TMEM92-AS1, promotes gastric cancer progression by binding to YBX1 to mediate CCL5. *Mol Oncol*. 2021;15(4):1256-1273.
19. Guo Y, Chen D, Su X, Chen J, Li Y. The lncRNA ELF3-AS1 promotes bladder cancer progression by interaction with Krüppel-like factor 8. *Biochem Biophys Res Commun*. 2019;508(3):762-768.
20. Zhang Z, Nong L, Chen M, et al. LncRNA ELF3-AS1 Promotes Nonsmall Cell Lung Cancer Cell Invasion and Migration by Downregulating miR-212. *Cancer Biother Radiopharm*. 2020;1–6.
21. Mei JC, Yan G, Mei SQ. Diagnostic and Prognostic Potentials of Long Noncoding RNA ELF3-AS1 in Glioma Patients. *Dis Markers*. 2020;18(2020):8871746.
22. Yuan J, Kang J, Yang M. Long non-coding RNA ELF3-antisense RNA 1 promotes osteosarcoma cell proliferation by upregulating Kruppel-like factor 12 potentially via methylation of the microRNA-205 gene. *Oncol Lett*. 2020;19(3):2475-2480.
23. Chu H, Li Z, Gan Z, Yang Z, Wu Z, Rong M. LncRNA ELF3-AS1 is involved in the regulation of oral squamous cell carcinoma cell proliferation by reprogramming glucose metabolism. *Onco Targets Ther*. 2019;22(12):6857-6863.
24. Song S, Li C, Sen LI, Gao H, Lan X, Xue Y. Derived neutrophil to lymphocyte ratio and monocyte to lymphocyte ratio may be better biomarkers forpredicting overall survival of patients with advanced gastric cancer. *OncoTargets and Therapy*. 2017;10:3145-3154.
25. Cheng X, Li Y, Tan J, et al. CCL20 and CXCL8 synergize to promote progression and poor survival outcome in patients with colorectal cancer by collaborative induction of the epithelial–mesenchymal transition. *Cancer Lett*. 2014;348(1–2):77-87.
26. Geuens T, Bouhy D, Timmerman V. The hnRNP family: Insights into their role in health and disease. *Hum Genet*. 2016;135:851-867.
27. Gallardo M, Hornbaker M, Zhang X, Hu P, Bueso-Ramos PS. Aberrant hnRNP K expression: All roads lead to cancer. *Cell Cycle*. 2016;15:1552-1557.
28. Barboro P, Ferrari N, Balbi C. Emerging roles of heterogeneous nuclear ribonucleoprotein K (hnRNP K) in cancer progression. *Cancer Lett*. 2014;352:152-159.
29. Bomsztyk K, Denisenko O, Ostrowski J. hnRNP K: One protein multiple processes. *BioEssays*. 2004;26:629-638.
30. Xu H, Xu Y, Liang X, Zeng W. The biological function of heterogeneous nuclear ribonucleoprotein K(hnRNP K) and its roles in spermatogenisis. *J Agric Biotechnol*. 2015;23:661-670.
31. Li D, Wang X, Mei H, et al. Long noncoding RNA pancEts-1 promotes neuroblastoma progression through hnRNPK mediated b-Catenin stabilization. *Mol Cell Biol*. 2018;78(5):1169-1183.
32. Gao T, Liu X, He B, Nie Z, Zhu C, Zhang P. Exosomal lncRNA 91H is associated with poor development in colorectal cancer by modifying HNRNPK expression. *Cancer Cell Int*. 2018;18(1):11.
33. Zhao X, Liu Y, Yu S. Long noncoding RNA AWPPH promotes hepatocellular carcinoma progression through YBX1 and serves as a prognostic biomarker. *Biochim Biophys Acta Mol Basis Dis*. 2017;1863(7):1805-1816.
34. Guerra-Calderas L, González-Barrios R, Herrera LA. The role of the histone demethylase KDM4A in cancer. *Cancer Genetics*. 2015;208(5):215-224.
35. Wu Q, Guo L, Jiang F, Li L, Li Z, Chen F. Analysis of the miRNA–mRNA–lncRNA networks in ER+ and ER− breast cancer cell lines. *J Cell Mol Med*. 2015;19(12):2874-2887.
36. Hanahan D, Weinberg RA. Hallmarks of cancer: the next generation. *Cell*. 2011;144:646-674.
37. Coussens LM, Werb Z. Inflammation and cancer. *Nature*. 2002;420:860-867.
38. Balkwill F, Mantovani A. Inflammation and cancer: back to Virchow? *Lancet*. 2001;357:539-545.
39. Song S, Cong X, Li F, Xue Y. The Fibrinogen to Mean Platelet Volume Ratio Can Predict Overall Survival of Patients with Non-Metastatic Gastric Cancer. *J Gastric Cancer*. 2018;18(4):368-378.
40. Stone RL, Nick AM, Mcneish IA, Balkwill F, Han HD, Bottsfordmiller J. Paraneoplastic thrombocytosis in ovarian cancer. *N Engl J Med*. 2012;2012(18):237-238.
41. Li J, Meng H, Bai Y, Wang K. Regulation of lncRNA and Its Role in Cancer Metastasis. *Oncol Res*. 2016;23(5):205-217.
42. Bhan A, Soleimani M, Mandal SS. Long Noncoding RNA and Cancer: A New Paradigm. *Cancer Res*. 2017;77(15):3965-3981.
43. Leyten GH, Hessels D, Jannink SA, et al. Prospective multicentre evaluation of PCA3 and TMPRSS2-ERG gene fusions as diagnostic and prognostic urinary biomarkers for prostate cancer. *Eur Urol*. 2014;65(3):534-542.
44. Muscella A, Vetrugno C, Marsigliante S. CCL20 promotes migration and invasiveness of human cancerous breast epithelial cells in primary culture[J]. *Mol Carcinog*. 2017;56(11):2461-2473.
45. Zeng W, Chang H, Ma M, Li Y. CCL20/CCR6 promotes the invasion and migration of thyroid cancer cells via NF-kappa B signaling-induced MMP-3 production. *Exp Mol Pathol*. 2014;97(1):184-190.
46. Li W, Liu H. CCL20-CCR6 Cytokine Network Facilitate Treg Activity in Advanced Grades and Metastatic Variants of Hepatocellular Carcinoma. *Scand J Immunol*. 2016;83(1):33-37.
47. Hernandez E. Poor prognosis associated with thrombocytosis in patients with cervical cancer. *Cancer*. 2015;69(12):2975-2977.
48. Hufnagel DH, Cozzi GD, Crispens MA, Beeghly-Fadiel A. Platelets, Thrombocytosis, and Ovarian Cancer Prognosis: Surveying the Landscape of the Literature. *Int J Mol Sci*. 2020;21(21):8169.

49. Ishizuka M, Nagata H, Takagi K, Iwasaki Y, Kubota K. Preoperative thrombocytosis is associated with survival after surgery for colorectal cancer. *J Surg Oncol*. 2012;106(7):887-891.
50. Haemmerle M, Stone RL, Menter DG, Afshar-Kharghan V, Sood AK. The Platelet Lifeline to Cancer: Challenges and Opportunities. *Cancer Cell*. 2018;33(6):965-983.
51. Zhou C, Su H, Dai H. Thrombopoietin is associated with a prognosis of gastric adenocarcinoma. *Revista da Associação Médica Brasileira*. 2020;66(5):590–595.
52. Zou Z, Fan X, Liu Y, Sun Y, Zhang X, Sun G, Li X, Xu S. Endogenous thrombopoietin promotes non-small-cell lung carcinoma cell proliferation and migration by regulating EGFR signalling. *Journal of Cellular and Molecular Medicine*. 2020;24(12):6644–6657.

SUPPORTING INFORMATION

Additional supporting information may be found online in the Supporting Information section.

How to cite this article: Song S, He X, Wang J, et al. ELF3-AS1 contributes to gastric cancer progression by binding to hnRNPK and induces thrombocytosis in peripheral blood. *Cancer Sci*. 2021;112:4553–4569. https://doi.org/10.1111/cas.15104